Metabolic Engineering 33 (2016) 109–118

Contents lists available at ScienceDirect

Metabolic Engineering

journal homepage: www.elsevier.com/locate/ymben

Regular Article

Genetic programming of catalytic *Pseudomonas putida* biofilms for boosting biodegradation of haloalkanes

Ilaria Benedetti, Víctor de Lorenzo*, Pablo I. Nikel

Systems and Synthetic Biology Program, Centro Nacional de Biotecnología (CNB-CSIC), Madrid 28049, Spain

ARTICLE INFO

Article history:
Received 2 September 2015
Received in revised form
2 October 2015
Accepted 19 November 2015
Available online 24 November 2015

Keywords:
Pseudomonas putida
Catalytic biofilm
Dehalogenase
Metabolic engineering
Biocatalysis
Synthetic morphology

ABSTRACT

Bacterial biofilms outperform planktonic counterparts in whole-cell biocatalysis. The transition between planktonic and biofilm lifestyles of the platform strain *Pseudomonas putida* KT2440 is ruled by a regulatory network controlling the levels of the trigger signal cyclic di-GMP (c-di-GMP). This circumstance was exploited for designing a genetic device that over-runs the synthesis or degradation of c-di-GMP – thus making *P. putida* to form biofilms at user's will. For this purpose, the transcription of either *yedQ* (diguanylate cyclase) or *yhjH* (c-di-GMP phoshodiesterase) from *Escherichia coli* was artificially placed under the tight control of a cyclohexanone-responsive expression system. The resulting strain was subsequently endowed with a synthetic operon and tested for 1-chlorobutane biodegradation. Upon addition of cyclohexanone to the culture medium, the thereby designed *P. putida* cells formed biofilms displaying high dehalogenase activity. These results show that the morphologies and physical forms of whole-cell biocatalysts can be genetically programmed while purposely designing their biochemical activity.

1. Introduction

Pseudomonas putida is an environmental, Gram-negative bacterium that ubiquitously colonizes soil and metabolizes a broad range of natural and synthetic organic compounds (Martins dos Santos et al., 2004; Nelson et al., 2002; Nikel, 2012; Nikel et al., 2014a, (2015a); Timmis, 2002). Because of their remarkable ability to degrade pollutants, *P. putida* strains are being extensively studied for a number of industrial and environmental uses (Martínez-García et al., 2014a, 2014b, 2014c, 2014d; Poblete-Castro et al., 2012). In particular, strain KT2440, a derivative of the toluene-degrading wild-type *P. putida* strain mt-2 (Bagdasarian et al., 1981), exhibits unusual (and attractive) traits such as growth on a broad range of recalcitrant compounds, tolerance to solvents, antibiotics, and heavy metals, and shows high reducing power availability. These qualities make *P. putida* a platform of choice for engineering harsh redox reactions on organic substrates (Nikel, 2012). A large variety of genetic tools have been developed over the years to analyze, clone, and manipulate the genes (and even the whole genome) of this bacterium for a suite of environmental and industrial applications (Martínez-García and de Lorenzo, 2012; Martínez-García et al., 2015; Nikel and de Lorenzo, 2013a, 2013b). Still, any catalytic activity engineered in a given bacterial host has to be delivered to the cognate substrate in a specific physical format that often determines the whole effectiveness of the process. Planktonic cells are usually very sensitive to the stressful conditions prevalent in a stirred tank bioreactor (Delvigne and Goffin, 2013), or other catalytic scenarios where cells are dispersed in a much larger volume of an aqueous medium. In contrast, biofilms of catalytic bacteria are advantageous over suspended cells not only in that physical proximity limits the unwanted diffusion of intermediates (Rosche et al., 2009), but also in that they exhibit a superior tolerance to physicochemical insults and harsh reaction conditions (D'Alvise et al., 2010; Karande et al., in press). Moreover, bacteria within a biofilm are known to display lower cell-to-cell variability than their planktonic counterparts and endure different types of stresses (Ackermann, 2013; Nikel et al., 2014b). Finally, cells adhered to hard surfaces, e.g., on porous solid carriers such as Raschig rings, allow for the operation of catalysts in packed column reactors (Halan et al., 2012; 2014).

Alas, most Laboratory-adapted *P. putida* strains produce thin and somewhat weak biofilms (Gjermansen et al., 2005, 2010). It is often the case that recurrent re-isolation of the same strain from liquid media inadvertently results in the enrichment of mutants that stick less to surfaces. Furthermore, the occurrence of biofilms is subject to a complex regulatory network that rotates around controlling intracellular levels of the secondary messenger cyclic diguanosine monophosphate (c-di-GMP). This small molecule governs the transition from planktonic to biofilm lifestyle (and

* Corresponding author at: Systems and Synthetic Biology Program, Centro Nacional de Biotecnología (CNB-CSIC), Darwin 3, Campus de Cantoblanco Madrid 28049, Spain. Tel: +34 91 585 4536, Fax: +34 91 585 4506.
E-mail address: vdlorenzo@cnb.csic.es (V. de Lorenzo).

http://dx.doi.org/10.1016/j.ymben.2015.11.004
1096-7176/

back) in a wide range of bacteria (Römling et al., 2013; Schirmer and Jenal, 2009), including *P. putida* and other Pseudomonads (Österberg et al., 2013; Tolker-Nielsen et al., 2000; Ueda and Saneoka, 2014). This situation happens by regulating cell adhesiveness through inhibition of flagellar movement and production of sticky exopolymeric substances (EPS) (Fazli et al., 2014; Flemming and Wingender, 2010). More than 40 proteins encoded in the *P. putida* genome contain GGDEF domains (diguanylate cyclase needed for c-di-GMP formation) or EAL domains (c-di-GMP phosphodiesterase) (Ausmees et al., 2001; Gjermansen et al., 2006; Simm et al., 2004), making biofilm formation an archetypal polygenic phenotype. When the merged cyclase activity is high, c-di-GMP increases, matrix material and EPS are produced and biofilm is formed (Hengge, 2009; Liang, 2015). In contrast, elevated phosphodiesterase activity leads to dispersal of the surface-stuck bacteria. This regulatory complexity results on very limited options for artificially controlling biofilm development (Caly et al., 2015; Schuster and Markx, 2014), as it would be desirable for engineering predictable catalysts and their formulation for industrial bioprocesses.

In this work, we have engineered two genes from *Escherichia coli*, encoding active GGDEF and EAL domains, to be transcribed in *P. putida* under the control of a cyclohexanone-inducible, tightly-regulated expression system purposely designed to suit this objective (Benedetti et al., 2015). We show below that the resulting construct altogether took over the endogenous regulatory network of c-di-GMP and allowed for controlled biofilm formation according to specific catalytic needs, e.g., for biodegradation of the environmental pollutant 1-chlorobutane. Specifically, we demonstrate that dehalogenation of the haloalkane increased by >2-fold by delivering the biochemical activity from the thereby induced biofilm as compared to the same setup with planktonic cells. These results accredit not only that the catalytic efficiency of a whole-cell biotransformation can change dramatically with its planktonic versus biofilm lifestyle, but also that the physical form and the morphology of the active biomass can be genetically programmed by implanting synthetic devices on endogenous regulatory networks.

2. Materials and methods

2.1. Bacterial strains and culture conditions

Bacterial strains used in this study are listed in Table 1. *E. coli* HB101, carrying plasmid pRK600, was used as a helper for triparental mating, and it was routinely grown in LB medium (Green and Sambrook, 2012). *P. putida* was incubated at 30 °C in M9 minimal medium (Green and Sambrook, 2012) added with $MgSO_4$ at 2 mM and either glucose or succinate at 0.4% (w/v) as the sole carbon source. Kanamycin (Km, 50 μg ml^{-1}), streptomycin (Sm, 80 μg ml^{-1}), cloramphenicol (Cm, 30 μg ml^{-1}), gentamicin (Gm, 10 μg ml^{-1}), and/or tetracycline (Tc, 15 μg ml^{-1}) were supplemented to the culture media when required. For haloalkane dehalogenase assays, cells were grown in low-chloride M9 minimal medium (M9C medium), containing $(NH_4)_2SO_4$ instead of NH_4Cl and Na_2SO_4 instead of NaCl (Nikel and de Lorenzo, 2013a). Growth was estimated by measuring the optical density at 600 nm (OD_{600}) after diluting the culture whenever needed. Flask cultures were set in 125-ml Erlenmeyer flasks containing culture medium up to one-fifth of their nominal volume. Static cultures were incubated with no shaking, and shaken-flask cultures were agitated at 170 rpm. Unless stated otherwise in the text, cyclohexanone and isopropyl-β-D-1-thiogalactopyranoside (IPTG) were added to the cultures to induce the ChnR- and LacI^Q-based expression systems, respectively, at 1 mM.

2.2. Assessment of colony morphology in Congo Red medium plates

The colony morphology of selected *P. putida* recombinant strains was assessed in Congo Red plates, i.e., M9 minimal medium

Table 1
Bacterial strains and plasmids used in this study.

Bacterial strain	Relevant characteristics[a]	Reference
Escherichia coli		
HB101	Helper strain; F$^-$ λ^- *hsdS20*(r_B– m_B–) *recA13 leuB6*(Am) *araC14* Δ(*gpt-proA*)*62 lacY1 galK2*(Oc) *xyl-5 mtl-1 thiE1 rpsL20*(Sm^R) *glnX44*(AS)	Boyer and Roulland-Dussoix (1969)
Pseudomonas putida		
KT2440	Wild-type strain derived from *P. putida* mt-2, cured of the pWW0 TOL plasmid	Bagdasarian et al. (1981)
KT2440 Δall-Φ	*P. putida* KT2440 derivative with prophage 1, prophage 4, prophage 3, and prophage 2 deleted	Martínez-García et al. (2014c)
KT2440 Δall-Φ GFP	*P. putida* KT2440 Δall-Φ derivative constitutively expressing *gfp2* as a chromosomal Tn*7* insertion ($P_{A1/04/03}$→ *gfp2*), Gm^R	Martínez-García et al. (2014c)
KT-BG	*P. putida* KT2440 derivative carrying a BCD2-*msf●GFP* transcriptional fusion as a chromosomal Tn*7* insertion, Gm^R	Zoebel et al. (in press)
KT-BG-PelA	*P. putida* KT-BG derivative carrying a P_{pelA}-BDC2-*msf●GFP* transcriptional fusion as a chromosomal Tn*7* insertion (cyclic diguanosine monophosphate reporter strain), Gm^R	This study
Plasmids		
pRK600	Cm^R; *oriV*(ColE1), *tra*$^+$ *mob*$^+$ functions from plasmid RK2	Keen et al. (1988)
pSEVA2311	Km^R; *oriV*(pBBR1), *chnR*, P_{chnB}	Benedetti et al. (2015)
pSEVA2311M	Km^R; *oriV*(pBBR1), *chnR*, P_{chnB} → *msf●GFP*	Benedetti et al. (2015)
pSEVA424	Sm^R; *oriV*(RK2), *lacI*^{Q}, P_{trc}	Silva-Rocha et al. (2013)
pYedQ	Tc^R; vector pRK404 (Scott et al., 2003) carrying *yedQ* from *E. coli*	Ausmees et al. (2001)
pYhjH	Tc^R; vector pBBR1-MCS3 (Kovach et al., 1995) carrying *yhjH* from *E. coli*	Gjermansen et al. (2006)
pSYedQ	Km^R; *oriV*(pBBR1), *chnR*, P_{chnB}→*yedQ*	This study
pSYhjH	Km^R; *oriV*(pBBR1), *chnR*, P_{chnB}→*yhjH*	This study
pSLacH	Km^R; *oriV*(pBBR1), *lacI*^{Q}, P_{trc}→*yhjH*	This study
pBG	Km^R Gm^R; *oriV*(R6K), carries the Tn*7* ends Tn7L and Tn7R and a BCD2-*msf●GFP* fusion	Zoebel et al. (in press)
pBG-PelA	Km^R Gm^R; pBG carrying the P_{pelA} promoter as a P_{pelA}-BDC2-*msf●GFP* transcriptional fusion	This study
pSEVA4413	Sm^R; *oriV*(ColE1), P_{EM7} promoter	This study
pAHDO	Sm^R; *oriV*(RK2), *xylS*, *Pm*→AHDO	Nikel and de Lorenzo (2013a)
pSAHDO	Sm^R; *oriV*(ColE1), P_{EM7}→AHDO	This study

[a] Abbreviations used in this table are as follows: Cm, chloramphenicol; Km, kanamycin; Gm, gentamycin; Rif, rifampicin; Sm, streptomycin; Tc, tetracycline; *gfp2*, gene encoding an enhanced green fluorescent protein; *msf●GFP*, gene encoding the monomeric and superfolder green fluorescent protein (msf●GFP); BCD2, optimized translational coupler; AHDO, alkyl halide degradation operon.

containing 0.4% (w/v) glucose, 1% (w/v) agar, 40 μg ml^{-1} Congo Red, and 20 μg ml^{-1} Coomassie brilliant blue G-250. For this assay, *P. putida* cells carrying the plasmids described in the text were grown for 18 h in M9 minimal medium containing 0.4% (w/v) glucose and supplemented with Km. These overnight cultures were washed by centrifugation and resuspension, and finally diluted to an OD_{600} of 0.05 in fresh M9 minimal medium (without any carbon source) and an aliquot of each bacterial suspension (5 μl) was spotted onto a fresh Congo Red plate. Cyclohexanone was provided as the inducer in the form of saturating vapors by placing a cyclohexanone-filled tip on the lid of the Petri dish. Bacterial strains were allowed to grow for 5 days at 30 °C until visible formation of aggregated colonies was evident by visual inspection of the Petri dishes (Ruiz et al., 2006). Pictures of individual colonies were acquired at 25 × and 500 × magnification by using a Leica DMR™ wide field microscope (Leica Microsystems GmbH, Wetzlar, Germany) with differential interference contrast optics, equipped with the Leica Twain™ software (Leica Microsystems GmbH) as described elsewhere (Nikel et al., 2015b). Images were processed with the ImageJ 1.46r software (http://imagej.nih.gov/ij/index.html).

2.3. DNA techniques and plasmid construction

All the plasmids used in this study are listed in Table 1. DNA amplification by PCR, digestion with restriction enzymes, ligation, and other standard cloning procedures followed well established protocols (Green and Sambrook, 2012) and specific instructions from the manufacturers. All plasmid constructs were confirmed by Sanger DNA sequencing (Secugen SL, Madrid, Spain).

2.3.1. Construction of plasmids for the regulated expression of genes encoding a diguanylate cyclase and a phoshodiesterase from E. coli

Expression plasmids for the tightly-regulated expression of genes influencing biofilm formation were constructed as follows. The gene encoding the YedQ cyclase was amplified by PCR from plasmid pYedQ using *yedQ*-F [5′-AAA CCT AGG TT*A GGA GGA* AAA ACA CGT GCA GCA CGA GAC AAA AAT G-3′, recognition site for *Avr*II underlined, synthetic Shine-Dalgarno (SD) sequence in italics] and *yedQ*-R (5′-AAA GAA TTC TTA AGC GTT ATC GCT CGC-3′, recognition site for *Eco*RI underlined), and cloned into pSEVA2311 as an *Avr*II/*Eco*RI fragment, yielding plasmid pSYedQ (Table 1). The gene encoding the YhjH phosphodiesterase was amplified by PCR from plasmid pYhjH using *yhjH*-F (5′-AAA GAG CTC TT*A GGA GGA* AAA ACA TAT GAT AAG GCA GGT TAT CC-3′, recognition site for *Sac*I underlined, synthetic SD sequence in italics) and *yhjH*-R (5′-AAA GGA TCC TTA TAG CGC CAG AAC CG-3′, recognition site for *Bam*HI underlined), and cloned into pSEVA2311 and pSEVA424 as a *Sac*I/*Bam*HI fragment, yielding plasmids pSYhjH and pSLacH, respectively (Table 1).

2.3.2. Construction of a synthetic operon for the degradation of alkyl halides

The synthetic operon *AHDO* (*A*lkyl *H*alide *D*egradation *O*peron) spans the genes encoding the DhaA and CaaD1/2 haloalkane dehalogenases from *Pseudomonas pavonaceae* strain 170 (Nikel et al., 2013b; Poelarends et al., 1998). The constitutive expression of *dhaA*, *caaD1*, and *caaD2* was attained by transferring a *Kpn*I/*Hin*dIII DNA fragment from the expression plasmid pAHDO (Table 1) into pSEVA4413, which carries the constitutive, synthetic P_{EM7} promoter, yielding plasmid pSAHDO. In pSAHDO, the expression of *dhaA*, *caaD1*, and *caaD2* is under transcriptional control of the P_{EM7} promoter to ensure appropriately high levels of dehalogenase activity in the recombinants.

2.3.3. Construction of a reporter P. putida strain for in vivo assessment of cyclic diguanosine monophosphate

P. putida KT-BG-PelA (Table 1), a strain used as a whole-cell biosensor to analyze the intracellular content of c-di-GMP, was constructed as follows. The P_{pelA} promoter of *Pseudomonas aeruginosa* PAO1, known to respond to the intracellular c-di-GMP concentration (Baraquet et al., 2012), was cloned as an *Avr*II/*Pac*I amplicon into the mini-Tn*7* vector pBG, thereby obtaining plasmid pBG-PelA. The synthetic Tn*7* transposon in this plasmid, bearing the P_{pelA}-BCD2-*msf●GFP* transcriptional fusion, was mobilized by tetraparental mating (Zoebel et al., in press) into the chromosome of wild-type *P. putida* KT2440, achieving *P. putida* KT-BG-PelA. To qualitatively estimate the intracellular concentration of c-di-GMP through the P_{pelA} promoter activity, plasmids pSEVA2311, pSYedQ, and pSYhjH were moved to *P. putida* KT-BG-PelA by triparental mating (Herrero et al., 1990). Recombinants were statically incubated overnight at 30 °C in M9 minimal medium supplemented with Km, glucose at 0.4% (w/v), and cyclohexanone at 1 mM. The msf●GFP signal was detected in the flasks by placing them on top of a Safe Imager™ 2.0 Blue Light Transilluminator (Thermo Fischer Scientific Inc., Waltham, MA, USA). Pictures were acquired under bright field or fluorescence with a Nikon D60 camera (Nikon Inc., Melville, NY, USA).

2.4. Single-cell analysis by flow cytometry

A MACSQuant™ VYB cytometer (Miltenyi Biotec, Bergisch Gladbach, Germany) was used for msf●GFP analysis and quantification as indicated elsewhere (Martínez-García et al., 2014a). An Ar laser, diode-pumped solid state, was used to excite msf●GFP at 488 nm and the fluorescence signal was recovered with a 525 ± 40 nm band-pass filter. To quantitatively estimate the intracellular concentration of c-di-GMP through the P_{pelA} promoter activity, plasmids pSEVA2311, pSYedQ, and pSYhjH were moved to *P. putida* KT-BG-PelA by triparental mating. Recombinants were statically incubated overnight at 30 °C in M9 minimal medium supplemented with Km, glucose at 0.4% (w/v), and cyclohexanone at 1 mM. An aliquot of these overnight cultures (1 ml) was washed three times with filtered 1 × phosphate buffered saline (1 × PBS; 8 g l^{-1} NaCl, 0.2 g l^{-1} KCl, 1.4 g l^{-1} Na_2HPO_4, and 0.2 g l^{-1} KH_2PO_4, pH 7.4), re-suspended with 1 × PBS and analyzed by flow cytometry. The flow cytometry analysis was executed on at least 20,000 cells from each sample and the corresponding data was processed using FlowJo v. 9.6.2 software (FlowJo LLC, Ashland, OR, USA).

2.5. Biofilm assays and fluorescence microscopy

Biofilm formation was quantified by means of the crystal violet assay (Nikel et al., 2013a; O'Toole and Kolter, 1998). Cells were grown in 96-well microtiter plates (Nunclon™Δ Surface; Nunc A/S, Roskilde, Denmark) in M9 minimal medium supplemented with the appropriate carbon sources and antibiotics, and with different inducer concentrations, and allowed to grow for 24 h at 30 °C without shaking. The culture broth was removed from the plates, and the OD_{600} was then measured in a 200-μl aliquot of the cell suspension in a SpectraMax Plus^{384} Microplate Reader (Molecular Devices, Sunnyvale, CA, USA). After washing wells three times with H_2O, 200 μl of a 0.1% (w/v) crystal violet solution was added to the plates, which were then incubated 30 min at room temperature. After discarding the solution, the remaining crystal violet associated with biofilms was dissolved by addition of 150 μl of a 33% (v/v) acetic acid solution. The plates were agitated gently for 1 h. Crystal violet density was acquired in a SpectraMax Plus^{384} Microplate Reader at 590 nm, and these values were normalized to the OD_{600} of each culture to obtain biofilm indexes. In another set

of experiments, a glass coverslip (22 mm × 22 mm; Menzel-Gläser GmbH, Braunschweig, Germany) was placed in a tilted position in a six-well plate (Thermo Fisher Scientific Inc., Pittsburgh, PA, USA) containing 5 ml of M9 minimal medium supplemented with glucose, the appropriate antibiotics, and cyclohexanone. Wells were inoculated with cells pre-grown in the same medium (in shaken-flask cultures) at an initial OD_{600} of 0.05. After incubating the plates at 30 °C without shaking during 24 h, coverslips were recovered and washed three times with H_2O. Each coverslip was assembled with a slide including Prolong™ (Life Technologies Corp., Grand Island, NY, USA) to suppress photobleaching, and sealed using clear nail polish. Coverslips were then washed with a 10% (w/v) sodium dodecyl sulfate solution to obtain a one-dimensional image of the biofilm surface. Microscopy was performed using an Olympus BX61 microscope equipped with a 100× phase contrast objective and a DP70 camera (Olympus Corp., Tokyo, Japan). GFP signals were measured using wide-field excitation with a MNIBA2 fluorescence mirror unit.

2.6. Haloalkane dehalogenase assay

P. putida recombinants were cultured in 96-well microtiter plates in M9C medium containing either 0.4% (w/v) glucose or succinate, 5 mM 1-chlorobutane, and the appropriate inducer and antibiotics for 48 h at 30 °C without shaking. Halide liberation was monitored colorimetrically by the method of Bergmann and Sanik (1957), with the modifications described by Nikel and de Lorenzo (2013a). This assay method depends on displacement of the thiocyanate ion from $Hg(SCN)_2$ by inorganic chloride. Halide production (in the 0–1 mM range) was determined spectrophotometrically at 460 nm. In order to normalize the haloalkane dehalogenase activity, the raw activity was normalized to the total protein in each well as follows. Dehalogenase activity was determined as indicated by Nikel and de Lorenzo (2013a) in a 200-µl aliquot of the culture broth and in the attached cells (i.e., biofilm) after removing all the liquid in the well. In parallel, the total protein concentration was determined in each fraction (i.e., planktonic and attached cells) as per the Bradford assay (Bradford, 1976) using a kit purchased from Bio-Rad Corp. (Hercules, CA, USA), after complete bacterial cell lysis using the BugBuster™ protein extraction reagent (Novagen™; Merck Millipore Corp., Billerica, MA, USA).

2.7. Chemicals and reagents

Unless stated otherwise, all chemicals and inducers were purchased from Sigma-Aldrich Co. (St. Louis, MO), while flow cytometry materials (buffers and calibration beads) were purchased from Miltenyi Biotec GmbH.

3. Results and discussion

3.1. Use of a cyclohexanone-responsive expression system to manipulate biofilm formation and dispersal in P. putida KT2440

Although *P. putida* KT2440 is a versatile host for engineering a variety of biotransformations, this strain is a poor and somewhat unpredictable biofilm former, a situation that can constitute a disadvantage for biotechnological applications (see Section 1). The work reported in this study aims at controlling the attachment of *P. putida* cells to solid surfaces for the sake of improving its catalytic abilities and easing its handling in consolidated bioprocesses. To this end, we developed and implanted a genetic plug-in device that takes over the native transcriptional and metabolic subnetworks of *P. putida* determining the synthesis and degradation of c-di-GMP. In this way, the intracellular levels of this second messenger (and therefore, the ability of the bacterium to form biofilms) become subjected to the deliberate addition of an exogenous signal (e.g., a chemical inducer). The vector of choice for this purpose was plasmid pSEVA2311, described by Benedetti et al. (2015), in which the cyclohexanone-responsive ChnR regulator and the P_{chnB} promoter from the Gram-negative bacterium *Acinetobacter johnsonii* have been standardized according to the SEVA (*S*tandard *E*uropean *V*ector *A*rchitecture) rules (Martínez-García et al., 2014b; Silva-Rocha et al., 2013). The output of the ChnR/P_{chnB} expression system has been parameterized in *E. coli* using a fluorescent reporter (Benedetti et al., 2015).

In order to improve the biofilm formation ability of *P. putida*, we decided to rewire the expression of a diguanylate cyclase gene by cloning *yedQ* from *E. coli* into pSEVA2311, and the resulting plasmid was termed pSYedQ (Table 1). In parallel, the same expression system was used to drive the expression of the phosphodiesterase YhjH, encoded by *yhjH* from *E. coli*, which was cloned in pSEVA2311 to yield a construct termed pSYhjH (Table 1). These two enzymes control the turnover of c-di-GMP in a fashion that would allow the user to modify the levels of this secondary messenger at will. In particular, YedQ, which contains a GGDEF domain, drives the formation of c-di-GMP from GTP; while YhjH, which contains an EAL domain, catalyzes the breakdown of c-di-GMP into 5′-phosphoguanylyl-(3′→5′)-guanosine (pGpG) and, ultimately, GMP (Fig. 1A). We transferred the plasmids (pSEVA2311, used as a control, pSYedQ, and pSYhjH) into *P. putida* KT2440 by triparental mating and confirmed their presence by antibiotic selection and digestion of plasmid DNA with appropriate restriction enzymes. In a first attempt to evaluate the functionality of YedQ, we grew *P. putida* KT2440/pSYedQ in M9 minimal medium containing glucose, and after 24 h of static incubation of the flasks, the attached cells were stained with crystal violet to qualitatively visualize biofilm formation (Fig. 1B). This simple test showed that the amount of biofilm formed by the recombinant carrying YedQ was more abundant that that formed by the control strain (i.e., *P. putida* KT2440/pSEVA2311), and that biofilm formation was even more evident in the culture incubated in the presence of cyclohexanone.

To quantitatively assess the function of the new plasmid constructs, we determined biofilm formation in the different strains at stake under glycolytic or gluconeogenic growth conditions. *P. putida* cells carrying either plasmid pSYedQ or vector pSEVA2311 were statically grown in glucose- or succinate-containing M9 minimal medium for 24 h in multi-well plates. Cells were either grown with no inducer or exposed to varying concentrations of cyclohexanone. Biofilm formation was quantified using the crystal violet assay. The results indicate that *P. putida* KT2440 bearing pSYedQ formed more biofilm than the control strain carrying the empty vector under all the conditions tested (Fig. 1C and D), and that the level of biofilm production was proportional to the concentration of the inducer. The formation of biofilm was slightly higher in succinate cultures than in the cultures amended with glucose. At the highest concentration of cyclohexanone used in these experiments (i.e., 5 mM), the biofilm index in glucose and succinate cultures for *P. putida* KT2440/pSYedQ was 1.8- and 2.1-fold higher than in uninduced cultures. Remarkably, the control *P. putida* strain carrying the empty pSEVA2311 vector formed the same amount of biofilm as did the uninduced recombinant expressing *yedQ*, which is a further indication of the low level of leaky expression of the ChnR/P_{chnB} expression system.

Expectedly, when biofilm formation was measured in cultures of *P. putida* KT2440 bearing pSYhjH (i.e., expressing the phosphodiesterase domain), the opposite effect was observed as that caused by YedQ: as the inducer concentration increased (which corresponds to increasingly higher phosphodiesterase activities),

the recombinants produced less biofilm (Fig. 1E and F). As indicated before, all the strains under examination had a higher biofilm-forming capability in the presence of succinate as the carbon source. The overexpression of *yhjH* in *P. putida* KT2440 at the highest concentration of cyclohexanone determined a decrease of 64% and 53% in the cell attachment in glucose and succinate cultures, respectively, as compared to uninduced control conditions. The effect of overproducing YhjH on biofilm dispersal seemed less prominent than that of YedQ in inducing cell attachment. One of the possible reasons for this observation is the known inhibition of some phosphodiesterase enzymes by product accumulation, particularly pGpG (Lacey et al., 2010). Finally, and to further evaluate the tightness of the ChnR/P_{chnB} expression system under these working conditions, we introduced an additional control in this set of experiments in which transcription of the *yhjH* phosphodiesterase was controlled by the commonly used LacI^{Q}/P_{trc} expression system (i.e., plasmid pSYLacH, see Table 1). Side-by-side comparison of these two expression systems evidenced a lower basal expression of ChnR/P_{chnB} as compared to that brought about by LacI^{Q}/P_{trc}, particularly in succinate cultures (Fig. 1E). In this case, biofilm formation by *P. putida* KT2440/pSYLacH decreased by 28% in the absence of IPTG. Besides the known leakiness of the LacI^{Q}/P_{trc} expression system, mounting experimental evidence point to a toxic effect of IPTG when this chemical is used as an inducer. Interestingly, we did not observe any compromise of the bacterial growth even when cyclohexanone was added at 5 mM as the inducer of the ChnR/P_{chnB} expression system (data not shown). Since all these experiments pointed to an enhanced biofilm formation profile when cells overproduce diguanylate cyclase, we next explored the micro- and macroscopic properties of *P. putida* cells overexpressing *yedQ* as explained in Section 3.2.

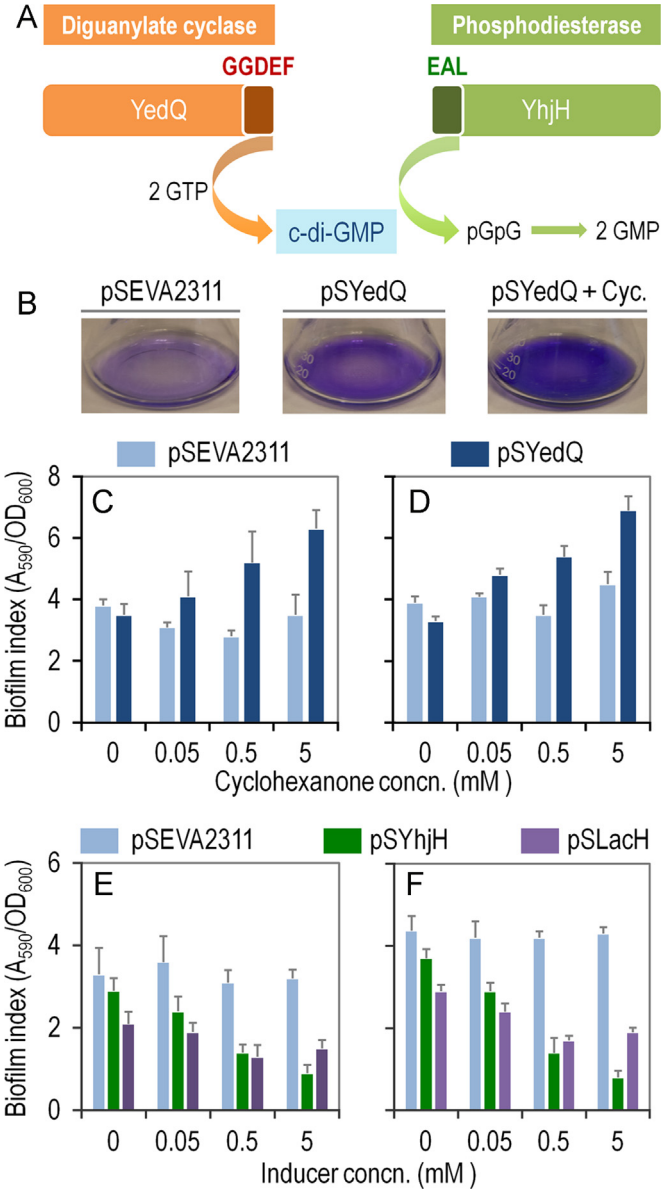

Fig. 1. Quantification of biofilm formation by *Pseudomonas putida* KT2440 carrying the YedQ diguanylate cyclase or the YhjH phosphodiesterase from *Escherichia coli* under control of the ChnR/P_{chnB} expression system. (A) The synthesis and hydrolysis of cyclic diguanosine monophosphate (c-di-GMP) is controlled by diguanylate cyclases, that convert two molecules of guanosine triphosphate (GTP) into c-di-GMP, and diesterases, that break down c-di-GMP to yield 5′-phosphoguanylyl-(3′→5′)-guanosine (pGpG) . This species is further converted into two molecules of guanosine monophosphate (GMP). In general, c-di-GMP is known to stimulate the biosynthesis of adhesins and expolysaccharide matrix substances in biofilms while inhibiting various forms of motility. The two enzymes used in this work are YedQ and YhjH from *Escherichia coli*, a diguanylate cyclase and a diesterase, respectively. YedQ bears a GGEDF domain and YhjH carries an EAL domain, which catalyze the synthesis and degradation of c-di-GMP, respectively. (B) Biofilm formation by *P. putida* KT2440 cells carrying either pSEVA2311 (empty plasmid) or pSYedQ (carrying the *yedQ* diguanylate cyclase under control of ChnR/P_{chnB}). Cells were grown in M9 minimal medium with 0.4% (w/v) glucose in static cultures for 24 h at 30 °C, after which the culture broth was removed and biofilms were visualized by staining the attached cells with crystal violet as detailed in Section 2. The ChnR/P_{chnB} system was induced by addition of cyclohexanone (Cyc.) at 1 mM at the onset of the cultivation. (C–F) Biofilm formation by different recombinant *P. putida* strains bearing pSEVA2311 (empty plasmid), pSYedQ (carrying the *yedQ* diguanylate cyclase under control of ChnR/P_{chnB}), pSYhjH (carrying the *yhjH* phosphodiesterase under control of ChnR/P_{chnB}), or pSLacH (carrying the *yhjH* phosphodiesterase under control of LacI^{Q}/P_{trc}) quantitatively assessed in microtiter plates. In all cases, cells were grown in M9 minimal medium in static cultures for 24 h at 30 °C using either glucose (C and E) or succinate (D and F) as the sole carbon source. Cyclohexanone or isopropyl-β-D-thiogalactopyranoside was used as the inducers of the ChnR/P_{chnB} and the LacI^{Q}/P_{trc} expression systems at the concentrations indicated in the figure. The biofilm index values were obtained by normalizing the absorbance of crystal violet at 590 nm (A_{590}) to the bacterial growth in each well (estimated as the optical density measured at 600 nm, OD_{600}). Bars represent the mean values of the corresponding parameter ± standard deviation of triplicate measurements from at least four independent experiments. Concn., concentration.

3.2. Microscopy analysis of biofilm formation and colony morphology in recombinant P. putida KT2440 overexpressing yedQ

To analyze biofilm structure by microscopy, we first introduced either plasmid pSYedQ or the control vector pSEVA2311 into *P. putida* KT2440 Δall-Φ GFP by triparental mating. This strain is a derivative of prophage-less *P. putida* KT2440 Δall-Φ, a robust and more viable bacterial *chassis* for several metabolic manipulations (Martínez-García et al., 2014c), which constitutively expresses *gfp2* from a chromosomal insertion – and consequently it can be easily visualized in fluorescence microscopy experiments. In terms of its intrinsic capability of biofilm formation, no major differences have been detected as compared with the parental KT2440 strain (Martínez-García et al., 2014c). Since *P. putida* KT2440 Δall-Φ GFP grows very well under glycolytic conditions, we adopted an assay in which glass coverslips were placed in M9 minimal medium supplemented with glucose and cyclohexanone at 1 mM and inoculated with a diluted culture of *P. putida* KT2440 Δall-Φ GFP/pSYedQ. Control experiments were carried in parallel with an uninduced recombinant and also with the same strain carrying the empty pSEVA2311 vector. After 48 h, coverslips of all the strains under inspection were removed and prepared for microscopy analysis. Fig. 2A shows phase contrast images (left column), and the same coverslip preparations visualized in the green fluorescence channel (right column). Overproduction of the YedQ diguanylate cyclase, controlled by the ChnR/P_{chnB} expression

system, induced the generation of more biofilm matrix material than the control strain carrying the empty vector. In particular, cultures exposed to cyclohexanone exhibited clear microcolonies along the preparation, which is a microscopic indication of the enhanced biofilm-formation capability of the strain over-expressing *yedQ* from *E. coli*.

Colony morphology in solid culture medium containing the diazo dye Congo Red provides a qualitative indication of the formation of cellulose and other exopolymeric materials. To evaluate the influence in matrix formation upon the regulated activity of diguanylate cyclase or phosphodiesterase, the appearance of macrocolonies of *P. putida* KT2440 carrying the empty pSEVA2311 vector, pSYedQ, or pSYhjH was inspected in Congo Red plates in the presence of saturating concentrations of cyclohexanone in the vapor phase (Fig. 2B). Observation of the corresponding colonies under 25× or 500× magnification indicates that the strain overproducing diguanylate cyclase is able to form more cellulose and exopolysaccharide materials than the control strain carrying pSEVA2311. This difference is featured in the lobulated rims of the colony boundaries and the appearance of spots on the colony. Besides, colonies of the YedQ$^+$ strain firmly attached to the culture medium surface and had a sticky consistence (data not shown). On the contrary, the YhjH$^+$ strain attached poorly to the surface, and formed loose colonies, with wider borders. Taken together, these results are in accordance with the quantification of biofilm formation using the crystal violet assay (Fig. 1B) and the results obtained by fluorescence microscopy of microcolonies in the coverslip (Fig. 2A). The assays described in the sections above accredit how the activities brought about by YedQ or YhjH influence *P. putida* attachment to abiotic surfaces and biofilm dispersal, respectively. Yet, what is the biochemical basis of these phenotypes in the recombinants?

3.3. Construction and evaluation of a c-di-GMP bioreporter P. putida strain

In bacteria, c-di-GMP is a second messenger involved in a broad spectrum of cellular processes such as the regulation of metabolic activities, cell differentiation, and photomorphogenesis. c-di-GMP is produced from two molecules of GTP by diguanylate cyclases and it is broken down to yield 5′-phosphoguanylyl-(3′-5)-guanosine (pGpG) by specific phosphodiesterases (Hengge, 2009; Römling et al., 2013); pGpG is subsequently split into two GMP molecules (Orr et al., 2015) (Fig. 1A). As stated before, diguanylate cyclase activity is associated with the presence of GGDEF domains in some proteins, while the c-di-GMP–specific phosphodiesterase activity is linked to EAL domains. Recent studies indicated that proteins with GGDEF/EAL domains and the actual concentration of c-di-GMP are the key factors dictating the regulation of cellular adhesiveness and biofilm formation in a range of bacteria, including *P. putida* (Almblad et al., 2015; Ausmees et al., 2001; Gjermansen et al., 2006; O'Toole et al., 2000; Pamp and Tolker-Nielsen, 2007; Simm et al., 2004; Tolker-Nielsen et al., 2000). In the experiments described up to this point, we designed plasmids pSYedQ and pSYhjH in which the activity of diguanylate cyclase or phosphodiesterase, respectively, was modulated by mean of the ChnR/P_{chnB} expression system. As a consequence of these manipulations, we obtained *P. putida* strains able to produce more or less biofilms. To confirm that over-production of either YedQ or YhjH can be traced to c-di-GMP formation and degradation, respectively, we adopted a biosensor *P. putida* strain in which the c-di-

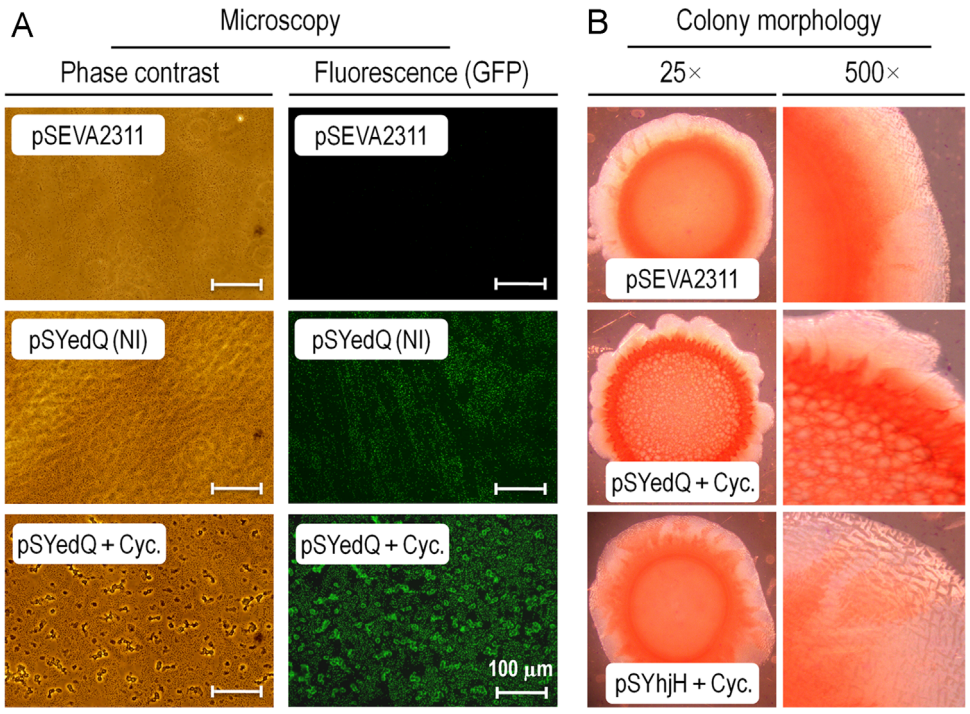

Fig. 2. Microscopy analysis of biofilm formation and colony morphology in response to the overproduction of the YedQ diguanylate cyclase from *Escherichia coli* in *Pseudomonas putida*. (A) Microscopy assessment of bacterial attachment to a glass surface. *P. putida* KT2440 Δall-Φ GFP bearing either pSEVA2311 (empty plasmid) or plasmid pSYedQ (carrying the *yedQ* diguanylate cyclase under control of ChnR/P_{chnB}) and was grown in M9 minimal medium containing 0.4% (w/v) glucose in presence or absence of cyclohexanone at 1 mM. A cover slide, which was placed in the culture medium inoculated with the cells, constituted the abiotic surface for biofilm attachment. Images were taken after 48 h of incubation at 30 °C without shaking. The cover slide was washed, cells were fixed, and observed under the optic microscope under both bright field and fluorescence. NI, non-induced; Cyc., cyclohexanone. (B) Macroscopic colony morphology in Congo Red plates. Cultures of *P. putida* KT2440 bearing either pSEVA2311 (empty plasmid), plasmid pSYedQ (carrying the *yedQ* diguanylate cyclase under control of ChnR/P_{chnB}), or plasmid pSYhjH (carrying the *yhjH* phosphodiesterase under control of ChnR/P_{chnB}) were diluted to an optical density measured at 600 nm of 0.05 and spotted onto Congo Red plates in the presence of saturating vapors of cyclohexanone. After 5 days of incubation at 30 °C, the colony morphology was analyzed by using a Leica DMR^{TM} wide field microscope at two different magnifications as indicated in the figure. Cyc., cyclohexanone.

GMP–responsive P_{pelA} promoter from *P. aeruginosa* (Baraquet et al., 2012) drives the expression of the reporter gene encoding msf●GFP (Fig. 3A). The functional cargo of such transcriptional fusion was delivered as a single copy into the chromosome of *P. putida* KT2440 by means of a synthetic, standardized version of the Tn*7* transposon (Zoebel et al., in press).

The simple visual inspection of cultures grown in M9 minimal medium containing glucose and 1 mM cyclohexanone under both bright field and blue light revealed that, while all the strains under study grew more or less similarly, *P. putida* KT2440/pSYedQ cells displayed considerably more fluorescence than the control strain carrying the empty pSEVA2311 vector (Fig. 3B). As expected, the YhjH$^+$ strain, overproducing the phosphodiesterase enzyme, had a lower fluorescence level than the other two recombinants. The quantification of the msf●GFP signal in these bacterial cultures by means of flow cytometry (Fig. 3C and D) confirmed the results described above. It is to be noticed that all the strains had an unimodal distribution of fluorescence within the entire bacterial population, thereby indicating an homogenous response of the biosensor device inserted as a monocopy of the target bacterium (Fig. 3C). The change in msf●GFP fluorescence between cyclohexanone-induced and uninduced cultures of the *P. putida* YdeQ$^+$ strain reached 25 fold, while for the *P. putida* recombinants carrying either the empty vector or the plasmid containing the *yhjH* diesterase the change was ~10 fold (Fig. 3D). It is plausible that overexpression of *yedQ* in this strain releases c-di-GMP to the intracellular pool of diffusible metabolites and small molecules which can reach and activate the biosensor device. In contrast, there may be a share of c-di-GMP which is protected by inactive GGDEF/EAL domains (Solano et al., 2009; Spurbeck et al., 2012), and, because of this, may not make it to the same pool and thus cannot be *seen* by the P_{pelA}–based biosensor. Still, even a conservative interpretation of the data of Fig. 3 indicated that, as expected, the alternative YedQ and YhjH production increases or decreases, respectively, the intracellular pool of c-di-GMP. This information sufficed for the design of a programmable, biofilm-forming catalytic *P. putida* strain as explained in Section 3.4.

3.4. Design of a catalytic biofilm for dehalogenation of haloalkanes

With the genetic device for controlling c-di-GMP levels in vivo in hand, *P. putida* KT2440 was subsequently used as the *chassis* to plug-in the genes that allow for degradation of xenobiotic haloalkanes such as 1-chlorobutane (Nikel et al., 2013b; Slater et al., 1997). As a first step, the synthetic *AHDO* (*a*lkyl *h*alide *d*egradation *o*peron) was assembled into vector pSEVA4413, to obtain plasmid pSAHDO, in which the genes encoding the dehalogenase activity are constitutively expressed by means of the P_{EM7} promoter (Fig. 4A). This operon spans three genes isolated from *P. pavonaceae* 170 encoding the enzymes responsible for degrading several halocompounds (Poelarends et al., 1998), and the corresponding dehalogenase activity was shown to be functional in *P. putida* KT2440 even under anoxic operating conditions (Nikel and de Lorenzo, 2013a). The enzymatic activities endowed by the *AHDO* operon are [i] a hydrolytic haloalkane dehalogenase (DhaA) with broad substrate specificity and [ii] the 3-chloroacrylic acid

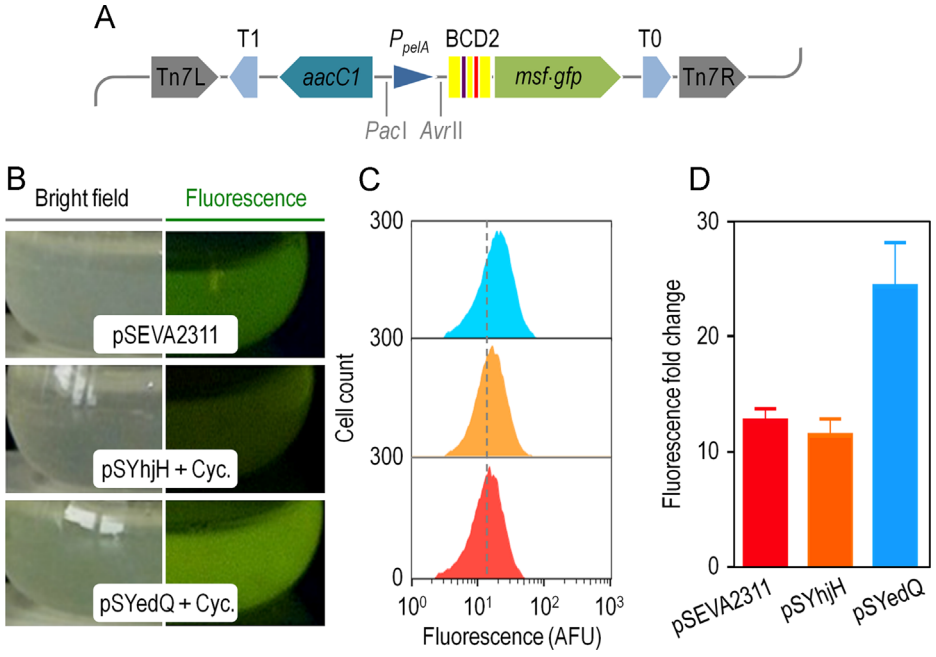

Fig. 3. Construction and validation of a fluorescence-based biosensor to assess the content of cyclic diguanosine-monophosphate (c-di-GMP) in vivo. (A) Structural organization of the relevant elements borne by *Pseudomonas putida* KT-BG-PelA. The functional elements inserted in the chromosome of this bacterium include [i] the Tn*7*L and Tn*7*R ends, which bracket the functional Tn*7* transposon, [ii] the T0 and T1 transcriptional terminators, which isolate the transcription of the Tn*7* transposon cargo from outside regulatory elements, [iii] the *aacC1* gene, which encodes the gentamicin-resistance determinant gentamicin 3′-acetyltransferase, [iv] the c-di-GMP-responsive P_{pelA} promoter, [v] the BCD2 optimized translational coupler, and [vi] the *msf●GFP* gene, which encodes the monomeric and superfolder green fluorescent protein. The elements in this outline are not drawn to scale. (B) Qualitative assessment of P_{pelA} promoter activity as a proxy of the c-di-GMP content in *P. putida* KT-BG-PelA. *P. putida* KT-BG-PelA carrying pSEVA2311 (empty plasmid), plasmid pSYedQ (carrying the *yedQ* diguanylate cyclase under control of ChnR/P_{chnB}), or plasmid pSYhjH (carrying the *yhjH* phosphodiesterase under control of ChnR/P_{chnB}) was statically grown for 24 h at 30 °C in M9 minimal medium containing 0.4% (w/v) glucose supplemented with the appropriate antibiotics and cyclohexanone at 1 mM. Flasks containing these cultures were photographed either under normal light or by placing them onto a blue light transilluminator. Cyc., cyclohexanone. (C) The msf●GFP fluorescence intensity in the strains described above was quantified by flow cytometry. The vertical dashed line represents the geometric *x*-mean value of the control strain (i.e., *P. putida* KT-BG-PelA carrying the empty pSEVA2311 plasmid). AFU, arbitrary fluorescence units. (D) Induction profile of P. putida KT-BG-PelA carrying pSEVA2311, pSYhjH, or pSYedQ in response to 1 mM cyclohexanone. Relative promoter output values were calculated by normalizing average fluorescence level of induced populations (i.e., geometric *x*-mean) to those of the untreated control samples (i.e., no cyclohexanone added). At least 20,000 cells were analyzed for each assay. Bars represent the mean values of the corresponding parameter ± standard deviation of triplicate measurements from at least four independent experiments.

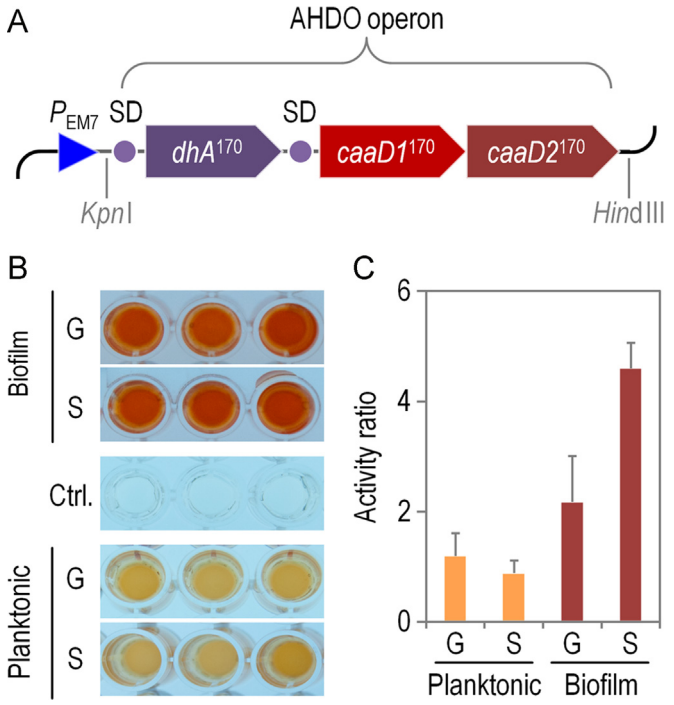

Fig. 4. Performance of the alkyl halide degradation operon (*AHDO*) in planktonic or surface-associated *Pseudomonas putida* cells. (A) Schematic representation of the synthetic operon in which $dhaA^{170}$, $caaD1^{170}$, and $caaD2^{170}$ are placed under control of the constitutive P_{EM7} promoter as a single transcriptional unit. The engineered organohalide biodegradation pathway is composed of enzymes from *P. pavonaceae* 170. The $dhaA^{170}$ and $caaD1$-$caaD2^{170}$ coding sequences were preceded by a Shine-Dalgarno (SD) motif. The elements in this outline are not drawn to scale. (B) Qualitative in vitro screening of haloalkane dehalogenase activity in wild-type *P. putida* KT2440 bearing plasmids pSYedQ (carrying the *yedQ* diguanylate cyclase under control of ChnR/P_{chnB}) and pSAHDO (carrying the *AHDO* operon under control of the constitutive P_{EM7} promoter). Cells were grown in M9C medium (a modified M9 minimal medium with low chloride content) supplemented with 0.4% (w/v) glucose (G) or succinate (S) and cyclohexanone at 1 mM. After 48 h of incubation at 30 °C without shaking, samples were prepared in order to obtain cells in planktonic conditions or in a biofilm state. These two fractions were exposed to a saturated 1-chlorobutane solution for 24 h. Dehalogenase activity was determined in vitro as indicated in Section 2, and plates were photographed as shown. *P. putida* KT2440 carrying plasmid pSAHDO and the empty pSEVA4413 vector were included in the assay to evaluate the background activity signal under control (Ctrl.) conditions. (C) In vitro quantification of the haloalkane dehalogenase activity in *P. putida* KT2440 recombinant cells growing in planktonic conditions and in a biofilm state. The specific activity ratio was calculated by dividing the values of enzyme activity obtained in either planktonic cells or in the biofilm of *P. putida* KT2440 carrying both pSYedQ and pSAHDO with the corresponding values obtained in *P. putida* KT2440 carrying pSYedQ and the empty pSEVA4413 vector. Bars represent the mean value of the enzyme activity ratio ± standard deviation of triplicate measurements from at least four independent experiments.

dehalogenase (CaaD), composed of two subunits, CaaD1 and CaaD2. DhaA and CaaD catalyze the complete dechlorination of several target compounds, such as 1-chlorobutane and 1,3-dichloropropene (Janssen, 2004). Haloalkane dehalogenases have a great biotechnological potential nowadays (Koudelakova et al., 2013). Plasmid pSAHDO was mobilized into *P. putida* KT2440 overproducing YedQ (i.e., the engineered biofilm-forming strain); as a control, we used the same strain carrying the empty pSEVA4413 vector (i.e., without the *dhaA*, *caaD1*, and *caaD2* genes). All the strains under examination were grown in microtiter multi-well plates in M9 minimal medium containing either glucose or succinate as the carbon source and supplemented with cyclohexanone at 1 mM. After 48 h of incubation without shaking, needed to establish a strong biofilm, a saturated 1-chlorobutane solution in water was separately added to planktonic cells and the biofilms. After an extra 24 h of incubation under the same conditions, planktonic cells and cells attached to the wells were assayed in vitro for dehalogenase activity (Fig. 4B and C). The bulk of dehalogenase activity was recovered in the biofilm fraction of all the cultures tested (Fig. 4B). The dehalogenase activity was normalized to the total protein concentration in each well (as an estimation of bacterial growth), and the resulting specific dehalogenase activity in *P. putida* KT2440 $YedQ^+$ $DhaA^+$ $CaaD1^+$ $CaaD2^+$, in turn, was compared to the specific activity displayed by *P. putida* KT2440 $YedQ^+$ carrying pSEVA4413 (Fig. 4C). In the planktonic fraction of cultures, this activity ratio was close to 1, which is an indication of a low dehalogenase activity in sessile cells irrespective of the carbon source used to grow the cells. In stark contrast, the biofilm fraction showed an activity ratio 2.1- or 4.3-fold higher in glucose and succinate cultures, respectively, than adherent cells carrying the empty pSEVA4413 vector. The levels of specific dehalogenase activity in the biofilm fraction ranged from 0.75–1.85 units mg protein^{-1}, which are comparable in magnitude to those previously reported when the expression of the *dhaA*, *caaD1*, and *caaD2* genes was controlled by using a XylS-*Pm*–based expression system (Nikel and de Lorenzo, 2013a).

4. Conclusion

While often considered deleterious in clinical settings, bacterial biofilms are of great interest in industrial and environmental Biotechnology. Applications of surface-attached biomass (e.g., in biocatalysis, during the removal of toxic metals, or in the formation of electricity in microbial fuel cells) are the subject of considerable attention in the last few years (Botyanszki et al., 2015; Cologgi et al., 2014; Halan et al., 2011; Li et al., 2013; Perni et al., 2013). This situation surely arises because biofilms allow for the delivery of the activity at stake in a concentrated physical form that is more manageable than bacteria in liquid suspension. Alas, the natural process of biofilm formation/dissolution is so complex that metabolic engineering has hardly contemplated to include this feature in any genetic design for improving catalytic efficiency. We show above that, regardless of the native and often unpredictable ability of *Pseudomonas* strains to produce biofilms, one can altogether submit this trait to the user's needs by artificially overtaking the endogenous network that manages intracellular c-di-GMP levels. We made that to happen by using an inducible and tightly controlled genetic device for heterologous expression of diaguanylate cyclase and phosphodiesterase genes. To the best of our knowledge, the work above is the first instance of *synthetic morphology* for the sake of biocatalysis, as the physical format of the biological material at issue has been changed in vivo in response to the activity of an implanted artificial gene network (Davies, 2008; Drubin et al., 2007; Tanaka and Yi, 2009).

On the bases outlined above, we could show that thereby generated biofilms boosted the ability of *P. putida* endowed with the synthetic operon *AHDO* to dehalogenate an archetypal haloalkane pollutant. In sum, we argue this work to be the first case in which the design of an optimal whole-cell catalyst merges [i] the genetic and biochemical assembly of the primary pathway (i.e., the *AHDO* operon) with [ii] its implantation in a bacterial host pre-evolved to sustain harsh reactions on tough substrates (*P. putida* KT2440), and [iii] its materialization in a physical form that eases its operation under working conditions. We believe that such physical form should in fact become an integral part of the design process of the genetically manufactured catalysts of the future.

Acknowledgments

The authors are indebted to Prof. D. Janssen (University of Groningen, The Netherlands) for his kind gift of *Pseudomonas pavonaceae* strain 170. We would like to also thank M. A. Hueso (CNB-CSIC, Spain) for her help in the construction of the *pelA*-based bioreporter strain. This work was supported by the CAM-BIOS Project of the Spanish Ministry of Economy and Competitiveness (RTC-2014-1777-3), the ST-FLOW (FP7-KBBE-2011-5-289326), EVOPROG (FP7-ICT-610730), ARISYS (ERC-2012-ADG-322797), and EmpowerPutida (EU-H2020-BIOTEC-2014-2015-6335536) Contracts of the European Union, and the PROMPT Project of the Autonomous Community of Madrid (CAM–S2010/BMD-2414). The authors declare that there is no conflict of interest.

References

Ackermann, M., 2013. Microbial individuality in the natural environment. ISME J. 7, 465–467.
Almblad, H., Harrison, J.J., Rybtke, M., Groizeleau, J., Givskov, M., Parsek, M., Tolker-Nielsen, T., 2015. The cyclic AMP-Vfr signaling pathway in *Pseudomonas aeruginosa* is inhibited by cyclic di-GMP. J. Bacteriol. 197, 2190–2200.
Ausmees, N., Mayer, R., Weinhouse, H., Volman, G., Amikam, D., Benziman, M., Lindberg, M., 2001. Genetic data indicate that proteins containing the GGDEF domain possess diguanylate cyclase activity. FEMS Microbiol. Lett. 204, 163–167.
Bagdasarian, M., Lurz, R., Rückert, B., Franklin, F.C.H., Bagdasarian, M.M., Frey, J., Timmis, K.N., 1981. Specific purpose plasmid cloning vectors. II. Broad host range, high copy number, RSF1010-derived vectors, and a host-vector system for gene cloning in *Pseudomonas*. Gene 16, 237–247.
Baraquet, C., Murakami, K., Parsek, M.R., Harwood, C.S., 2012. The FleQ protein from *Pseudomonas aeruginosa* functions as both a repressor and an activator to control gene expression from the *pel* operon promoter in response to c-di-GMP. Nucleic Acids Res. 40, 7207–7218.
Benedetti, I., Nikel, P.I., de Lorenzo, V., 2015. Standardization of a cyclohexanone-responsive expression system for Gram-negative bacteria. Data in Brief, Submitted for publication.
Bergmann, J.G., Sanik, J., 1957. Determination of trace amounts of chlorine in naphtha. Anal. Chem. 29, 241–243.
Botyanszki, Z., Tay, P.K., Nguyen, P.Q., Nussbaumer, M.G., Joshi, N.S., 2015. Engineered catalytic biofilms: site-specific enzyme immobilization onto *E. coli* curli nanofibers. Biotechnol. Bioeng. 112, 2016–2024.
Boyer, H.W., Roulland-Dussoix, D., 1969. A complementation analysis of the restriction and modification of DNA in *Escherichia coli*. J. Mol. Biol. 41, 459–472.
Bradford, M.M., 1976. A rapid and sensitive method for the quantitation of microgram quantities of protein utilizing the principle of protein-dye binding. Anal. Biochem. 72, 248–254.
Caly, D.L., Bellini, D., Walsh, M.A., Dow, J.M., Ryan, R.P., 2015. Targeting cyclic di-GMP signalling: a strategy to control biofilm formation? Curr. Pharm. Des. 21, 12–24.
Cologgi, D.L., Speers, A.M., Bullard, B.A., Kelly, S.D., Reguera, G., 2014. Enhanced uranium immobilization and reduction by *Geobacter sulfurreducens* biofilms. Appl. Environ. Microbiol. 80, 6638–6646.
D'Alvise, P.W., Sjøholm, O.R., Yankelevich, T., Jin, Y., Wuertz, S., Smets, B.F., 2010. TOL plasmid carriage enhances biofilm formation and increases extracellular DNA content in *Pseudomonas putida* KT2440. FEMS Microbiol. Lett. 312, 84–92.
Davies, J.A., 2008. Synthetic morphology: prospects for engineered, self-constructing anatomies. J. Anat. 212, 707–719.
Delvigne, F., Goffin, P., 2013. Microbial heterogeneity affects bioprocess robustness: dynamic single-cell analysis contributes to understanding of microbial populations. Biotechnol. J. 9, 61–72.
Drubin, D.A., Way, J.C., Silver, P.A., 2007. Designing biological systems. Genes Dev. 21, 242–254.
Fazli, M., Almblad, H., Rybtke, M.L., Givskov, M., Eberl, L., Tolker-Nielsen, T., 2014. Regulation of biofilm formation in *Pseudomonas* and *Burkholderia* species. Environ. Microbiol. 16, 1961–1981.
Flemming, H.C., Wingender, J., 2010. The biofilm matrix. Nat. Rev. Microbiol. 8, 623–633.
Gjermansen, M., Ragas, P., Sternberg, C., Molin, S., Tolker-Nielsen, T., 2005. Characterization of starvation-induced dispersion in *Pseudomonas putida* biofilms. Environ. Microbiol. 7, 894–906.
Gjermansen, M., Ragas, P., Tolker-Nielsen, T., 2006. Proteins with GGDEF and EAL domains regulate *Pseudomonas putida* biofilm formation and dispersal. FEMS Microbiol. Lett. 265, 215–224.
Gjermansen, M., Nilsson, M., Yang, L., Tolker-Nielsen, T., 2010. Characterization of starvation-induced dispersion in *Pseudomonas putida* biofilms: genetic elements and molecular mechanisms. Mol. Microbiol. 75, 815–826.
Green, M.R., Sambrook, J., 2012. Molecular cloning: a laboratory manual. Cold Spring Harbor Laboratory Press, Cold Spring Harbor, NY, USA.
Halan, B., Schmid, A., Buehler, K., 2011. Real-time solvent tolerance analysis of *Pseudomonas* sp. strain VLB120DC catalytic biofilms. Appl. Environ. Microbiol. 77, 1563–1571.
Halan, B., Buehler, K., Schmid, A., 2012. Biofilms as living catalysts in continuous chemical syntheses. Trends Biotechnol. 30, 453–465.
Halan, B., Letzel, T., Schmid, A., Buehler, K., 2014. Solid support membrane-aerated catalytic biofilm reactor for the continuous synthesis of (*S*)-styrene oxide at gram scale. Biotechnol. J. 9, 1339–1349.
Hengge, R., 2009. Principles of c-di-GMP signalling in bacteria. Nat. Rev. Microbiol. 7, 263–273.
Herrero, M., de Lorenzo, V., Timmis, K.N., 1990. Transposon vectors containing non-antibiotic resistance selection markers for cloning and stable chromosomal insertion of foreign genes in Gram-negative bacteria. J. Bacteriol. 172, 6557–6567.
Janssen, D.B., 2004. Evolving haloalkane dehalogenases. Curr. Opin. Chem. Biol. 8, 150–159.
Karande, R., Debor, L., Salamanca, D., Bogdahn, F., Engesser, K., Buehler, K., Schmid, A., 2015. Continuous cyclohexane oxidation to cyclohexanol using a novel cytochrome P450 monooxygenase from *Acidovorax* sp. CHX100 in recombinant *P. taiwanensis* VLB120 biofilms. Biotechnol. Bioeng. http://dxdoi.org/10.1002/bit.25696 (in press)
Keen, N.T., Tamaki, S., Kobayashi, D., Trollinger, D., 1988. Improved broad-host-range plasmids for DNA cloning in Gram-negative bacteria. Gene 70, 191–197.
Koudelakova, T., Bidmanova, S., Dvorak, P., Pavelka, A., Chaloupkova, R., Prokop, Z., Damborsky, J., 2013. Haloalkane dehalogenases: biotechnological applications. Biotechnol. J. 8, 32–45.
Kovach, M.E., Elzer, P.H., Hill, D.S., Robertson, G.T., Farris, M.A., Roop, R.M., Peterson, K.M., 1995. Four new derivatives of the broad-host-range cloning vector pBBR1MCS, carrying different antibiotic-resistance cassettes. Gene 166, 175–176.
Lacey, M.M., Partridge, J.D., Green, J., 2010. *Escherichia coli* K-12 YfgF is an anaerobic cyclic di-GMP phosphodiesterase with roles in cell surface remodelling and the oxidative stress response. Microbiology 156, 2873–2886.
Li, X.Z., Hauer, B., Rosche, B., 2013. Catalytic biofilms on structured packing for the production of glycolic acid. J. Microbiol. Biotechnol. 23, 195–204.
Liang, Z.X., 2015. The expanding roles of c-di-GMP in the biosynthesis of exopolysaccharides and secondary metabolites. Nat. Prod. Rep. 32, 663–683.
Martínez-García, E., de Lorenzo, V., 2012. Transposon-based and plasmid-based genetic tools for editing genomes of Gram-negative bacteria. Methods Mol. Biol. 813, 267–283.
Martínez-García, E., Aparicio, T., de Lorenzo, V., Nikel, P.I., 2014a. New transposon tools tailored for metabolic engineering of Gram-negative microbial cell factories. Front. Bioeng. Biotechnol. 2, 46.
Martínez-García, E., Aparicio, T., Goñi-Moreno, A., Fraile, S., de Lorenzo, V., 2014b. SEVA 2.0: an update of the Standard European Vector Architecture for de-/reconstruction of bacterial functionalities. Nucleic Acids Res. 43, D1183–D1189.
Martínez-García, E., Jatsenko, T., Kivisaar, M., de Lorenzo, V., 2014c. Freeing *Pseudomonas putida* KT2440 of its proviral load strengthens endurance to environmental stresses. Environ. Microbiol. 17, 76–90.
Martínez-García, E., Nikel, P.I., Aparicio, T., de Lorenzo, V., 2014d. *Pseudomonas* 2.0: genetic upgrading of *P. putida* KT2440 as an enhanced host for heterologous gene expression. Microb. Cell Factories 13, 159.
Martínez-García, E., Benedetti, I., Hueso, A., de Lorenzo, V., 2015. Mining environmental plasmids for synthetic biology parts and devices. Microbiol. Spectr. 3, PLAS-0033-2014.
Martins dos Santos, V.A.P., Heim, S., Moore, E.R., Strätz, M., Timmis, K.N., 2004. Insights into the genomic basis of niche specificity of *Pseudomonas putida* KT2440. Environ. Microbiol. 6, 1264–1286.
Nelson, K.E., Weinel, C., Paulsen, I.T., Dodson, R.J., Hilbert, H., Martins dos Santos, V. A.P., Fouts, D.E., Gill, S.R., Pop, M., Holmes, M., Brinkac, L., Beanan, M., DeBoy, R. T., Daugherty, S., Kolonay, J., Madupu, R., Nelson, W., White, O., Peterson, J., Khouri, H., Hance, I., Chris Lee, P., Holtzapple, E., Scanlan, D., Tran, K., Moazzez, A., Utterback, T., Rizzo, M., Lee, K., Kosack, D., Moestl, D., Wedler, H., Lauber, J., Stjepandic, D., Hoheisel, J., Straetz, M., Heim, S., Kiewitz, C., Eisen, J.A., Timmis, K.N., Düsterhöft, A., Tümmler, B., Fraser, C.M., 2002. Complete genome sequence and comparative analysis of the metabolically versatile *Pseudomonas putida* KT2440. Environ. Microbiol. 4, 799–808.
Nikel, P.I., 2012. A brief guide to *Pseudomonas putida* as a microbial cell factory. BioEssays, Available on line at: ⟨http://goo.gl/DXF1y⟩.
Nikel, P.I., de Lorenzo, V., 2013a. Engineering an anaerobic metabolic regime in *Pseudomonas putida* KT2440 for the anoxic biodegradation of 1,3-dichloroprop-1-ene. Metab. Eng. 15, 98–112.
Nikel, P.I., de Lorenzo, V., 2013b. Implantation of unmarked regulatory and metabolic modules in Gram-negative bacteria with specialised mini-transposon delivery vectors. J. Biotechnol. 163, 143–154.
Nikel, P.I., Chavarría, M., Martínez-García, E., Taylor, A.C., de Lorenzo, V., 2013a. Accumulation of inorganic polyphosphate enables stress endurance and catalytic vigour in *Pseudomonas putida* KT2440. Microb. Cell Factories 12, 50.
Nikel, P.I., Pérez-Pantoja, D., de Lorenzo, V., 2013b. Why are chlorinated pollutants so difficult to degrade aerobically? Redox stress limits 1,3-dichloroprop-1-ene metabolism by *Pseudomonas pavonaceae*. Philos. Trans. R. Soc. Lond. B: Biol. Sci. 368, 20120377.

Nikel, P.I., Martínez-García, E., de Lorenzo, V., 2014a. Biotechnological domestication of pseudomonads using synthetic biology. Nat. Rev. Microbiol. 12, 368–379.
Nikel, P.I., Silva-Rocha, R., Benedetti, I., de Lorenzo, V., 2014b. The private life of environmental bacteria: pollutant biodegradation at the single cell level. Environ. Microbiol. 16, 628–642.
Nikel, P.I., Chavarría, M., Fuhrer, T., Sauer, U., de Lorenzo, V., 2015a. *Pseudomonas putida* KT2440 strain metabolizes glucose through a cycle formed by enzymes of the Entner-Doudoroff, Embden-Meyerhof-Parnas, and pentose phosphate pathways. J. Biol. Chem. 290, 25920–25932.
Nikel, P.I., Romero-Campero, F.J., Zeidman, J.A., Goñi-Moreno, A., de Lorenzo, V., 2015b. The glycerol-dependent metabolic persistence of *Pseudomonas putida* KT2440 reflects the regulatory logic of the GlpR repressor. mBio 6, e00340–00315.
O'Toole, G., Kaplan, H.B., Kolter, R., 2000. Biofilm formation as microbial development. Annu. Rev. Microbiol. 54, 49–79.
O'Toole, G.A., Kolter, R., 1998. Flagellar and twitching motility are necessary for *Pseudomonas aeruginosa* biofilm development. Mol. Microbiol. 30, 295–304.
Orr, M.W., Donaldson, G.P., Severin, G.B., Wang, J., Sintim, H.O., Waters, C.M., Lee, V. T., 2015. Oligoribonuclease is the primary degradative enzyme for pGpG in *Pseudomonas aeruginosa* that is required for cyclic-di-GMP turnover. Proc. Natl. Acad. Sci. USA 112, E5048–EE5057.
Österberg, S., Åberg, A., Herrera Seitz, M.K., Wolf-Watz, M., Shingler, V., 2013. Genetic dissection of a motility-associated c-di-GMP signalling protein of *Pseudomonas putida*. Environ. Microbiol. Rep. 5, 556–565.
Pamp, S.J., Tolker-Nielsen, T., 2007. Multiple roles of biosurfactants in structural biofilm development by *Pseudomonas aeruginosa*. J. Bacteriol. 189, 2531–2539.
Perni, S., Hackett, L., Goss, R.J.M., Simmons, M.J., Overton, T.W., 2013. Optimisation of engineered *Escherichia coli* biofilms for enzymatic biosynthesis of L-halotryptophans. AMB Express 3, 66.
Poblete-Castro, I., Becker, J., Dohnt, K., Martins dos Santos, V.A.P., Wittmann, C., 2012. Industrial biotechnology of *Pseudomonas putida* and related species. Appl. Microbiol. Biotechnol. 93, 2279–2290.
Poelarends, G.J., Wilkens, M., Larkin, M.J., van Elsas, J.D., Janssen, D.B., 1998. Degradation of 1,3-dichloropropene by *Pseudomonas cichorii* 170. Appl. Environ. Microbiol. 64, 2931–2936.
Römling, U., Galperin, M.Y., Gomelsky, M., 2013. Cyclic di-GMP: the first 25 years of a universal bacterial second messenger. Microbiol. Mol. Biol. Rev. 77, 1–52.
Rosche, B., Li, X.Z., Hauer, B., Schmid, A., Buehler, K., 2009. Microbial biofilms: a concept for industrial catalysis? Trends Biotechnol. 27, 636–643.
Ruiz, J.A., Fernández, R.O., Nikel, P.I., Méndez, B.S., Pettinari, M.J., 2006. *dye (arc)* Mutants: insights into an unexplained phenotype and its suppression by the synthesis of poly(3-hydroxybutyrate) in *Escherichia coli* recombinants. FEMS Microbiol. Lett. 258, 55–60.
Schirmer, T., Jenal, U., 2009. Structural and mechanistic determinants of c-di-GMP signalling. Nat. Rev. Microbiol. 7, 724–735.
Schuster, J.J., Markx, G.H., 2014. Biofilm architecture. Adv. Biochem. Eng. Biotechnol. 146, 77–96.
Scott, H.N., Laible, P.D., Hanson, D.K., 2003. Sequences of versatile broad-host-range vectors of the RK2 family. Plasmid 50, 74–79.
Silva-Rocha, R., Martínez-García, E., Calles, B., Chavarría, M., Arce-Rodríguez, A., de las Heras, A., Páez-Espino, A.D., Durante-Rodríguez, G., Kim, J., Nikel, P.I., Platero, R., de Lorenzo, V., 2013. The Standard European Vector Architecture (SEVA): a coherent platform for the analysis and deployment of complex prokaryotic phenotypes. Nucleic Acids Res. 41, D666–D675.
Simm, R., Morr, M., Kader, A., Nimtz, M., Römling, U., 2004. GGDEF and EAL domains inversely regulate cyclic di-GMP levels and transition from sessility to motility. Mol. Microbiol. 53, 1123–1134.
Slater, J., Bull, A., Hardman, D., 1997. Microbial dehalogenation of halogenated alkanoic acids, alcohols and alkanes. Adv. Microb. Physiol. 38, 133–176.
Solano, C., García, B., Latasa, C., Toledo-Arana, A., Zorraquino, V., Valle, J., Casals, J., Pedroso, E., Lasa, I., 2009. Genetic reductionist approach for dissecting individual roles of GGDEF proteins within the c-di-GMP signaling network in *Salmonella*. Proc. Natl. Acad. Sci. USA 106, 7997–8002.
Spurbeck, R.R., Tarrien, R.J., Mobley, H.L., 2012. Enzymatically active and inactive phosphodiesterases and diguanylate cyclases are involved in regulation of motility or sessility in *Escherichia coli* CFT073. mBio 3, e00307–e00312.
Tanaka, H., Yi, T.M., 2009. Synthetic morphology using alternative inputs. PLoS One 4, e6946.
Timmis, K.N., 2002. *Pseudomonas putida*: a cosmopolitan opportunist *par excellence*. Environ. Microbiol. 4, 779–781.
Tolker-Nielsen, T., Brinch, U.C., Ragas, P.C., Andersen, J.B., Jacobsen, C.S., Molin, S., 2000. Development and dynamics of *Pseudomonas* sp. biofilms. J. Bacteriol. 182, 6482–6489.
Ueda, A., Saneoka, H., 2014. Characterization of the ability to form biofilms by plant-associated *Pseudomonas* species. Curr. Microbiol. 70, 506–513.
Zoebel, S., Benedetti, I., Eisenbach, L., de Lorenzo, V., Wierckx, N., Blank, L.M., 2015. Tn*7*-based device for calibrated heterologous gene expression in *Pseudomonas putida*. ACS. Synth. Biol. http://dxdoi.org/10.1021/acssynbio.1025b00058 (in press)